

INVITED REVIEW

Principles of sound production in wind instruments

Seiji Adachi*

ATR Human Information Science Laboratories,
Keihanna Science City, Kyoto, 619-0288 Japan

Abstract: This paper presents an outline of the sound production mechanisms in wind instruments and reviews recent progress in the research on different types of wind instruments, i.e., reed woodwinds, brass, and air-jet driven instruments. Until recently, sound production has been explained by models composed of lumped elements, each of which is often assumed to have only a few degrees of freedom. Although these models have achieved great success in understanding the fundamental properties of the instruments, recent experiments using elaborate methods of measurement, such as visualization, have revealed phenomena that cannot be explained by such models. To advance our understanding, more minute models with a large degree of freedom should be constructed as necessary. The following three different phenomena may be involved in sound production: mechanical oscillation of the reed, fluid dynamics of the airflow, and acoustic resonance of the instrument. Among them, our understanding of fluid dynamics is the most primitive, although it plays a crucial role in linking the sound generator with the acoustic resonator of the instrument. Recent research has also implied that a rigorous treatment of fluid dynamics is necessary for a thorough understanding of the principles of sound production in wind instruments.

Keywords: Self-excited oscillation, Nonlinearity, Aerodynamics, Multi-dimension

PACS number: 43.75.Ef, 43.75.Fg, 43.75.Np [DOI: 10.1250/ast.25.400]

1. INTRODUCTION

The sounding of wind instruments is a self-excited oscillation. The sound production system comprises the two major elements shown in Fig. 1. One is the sound generator, which includes the dynamics of reed vibration and air flowing through a reed aperture for reed woodwind instruments and brass instruments, or of an air jet deflected by sound for air-jet driven instruments. The other element is the sound resonator, that is, the air-column resonance of the instruments. These two elements interact with each other. In a reed woodwind instrument, a flow modulated by the reed in the generator enters the resonator and excites an oscillation of the air column. As a response, the resonator generates sound pressure at the entrance. This pressure acts as an external force on the reed and influences the oscillation. In this manner, the sound production system forms a feedback loop. If the loop gain becomes positive and overcomes losses such as the acoustic radiation, the system yields a self-excited oscillation or sounding. The energy maintaining the oscillation is provided by the air from the player's respiratory system.

The generator shows nonlinear behavior because it contains mechanical oscillation of the reed that may

include collision and fluid dynamics that is innately nonlinear. On the other hand, the resonator is very nearly linear except for special cases such as *fortissimo* played on the trombone [1]. It is nonlinearity that determines the characteristics of the generated sound such as the sound pressure level and harmonic structure.

McIntyre, Schumacher and Woodhouse proposed the simplest physical model where not only the sounding of wind instruments but also that of bowed string instruments can be treated in a unified manner [2]. In the first half of this paper, the principles of sound production in wind instruments are outlined by following their model. In the last half, recent progress in research on sound production is reviewed. Consequently, it becomes clear that both experimental and theoretical examinations of fluid dynamics are necessary to further investigate the sounding principles.

2. MCINTYRE-SCHUMACHER-WOODHOUSE MODEL

2.1. Generator

Complex phenomena related to reed vibration and the surrounding air occur in a clarinet mouthpiece. When the sounding is treated as a lumped system, however, it is sufficient to know the generator function $U = F(p)$, which shows the volume flow rate $U(t)$ at which the air flows into

*e-mail: sadachi@atr.jp

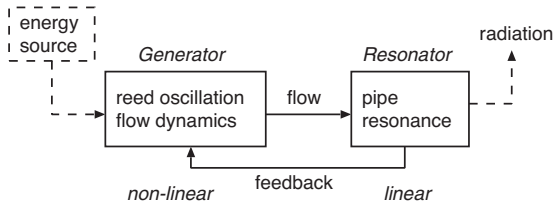


Fig. 1 Block diagram of sounding in a wind instrument.

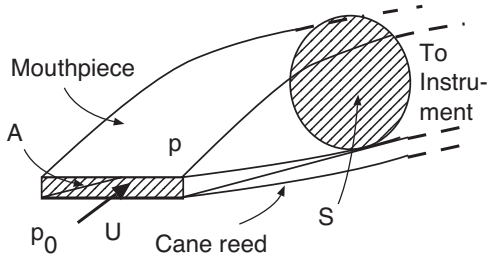


Fig. 2 Schematic diagram of clarinet mouthpiece.

the instrument for pressure $p(t)$ generated at the mouthpiece.

Figure 2 depicts a schematic diagram of a clarinet mouthpiece. When the blowing pressure is p_0 , a pressure difference $p_0 - p(t)$ occurs at the reed aperture, which results in generating an airflow through it. The pressure difference also changes the area of the reed aperture.

To model the generator function in the simplest way, the following assumptions are made: (1) The reed is a linear spring, and the area of the reed aperture is proportional to the pressure difference. (2) The airflow through the aperture is governed by Bernoulli's law. We then have

$$U = F(p) = A(p) \sqrt{\frac{2(p_0 - p)}{\rho}}$$

$$= bx_0 \frac{p - p_0 + p_c}{p_c} \sqrt{\frac{2(p_0 - p)}{\rho}}, \quad (1)$$

where $A(p)$ is the area of the aperture, and p_c is the pressure difference needed for the complete closure of the reed. The modeled generator function is illustrated by the thick line in Fig. 3. When the mouthpiece pressure p is equal to the blowing pressure p_0 , flow velocity vanishes and the volume flow rate becomes zero. As p is decreased, flow velocity increases with a rate proportional to the square root of the pressure decrease in accordance with Bernoulli's law. Then, U also increases. As p is further decreased, the reed is pushed toward the mouthpiece by a larger pressure difference, and the reed begins to close. This results in a decrease of U . When p is equal to or smaller than $p_0 - p_c$, the reed is closed completely, and U becomes zero.

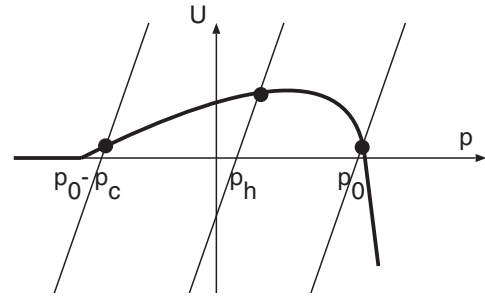


Fig. 3 Modeled generator function of clarinet.

2.2. Resonator

The resonator can be represented by the reflection function $r(t)$, which is defined as an incoming pressure wave that results from a pressure impulse injected into the entrance of the instrument. In principle, $r(t)$ has all of the information about the resonance of the instrument. When an outgoing pressure wave $p^+(t)$ is injected instead of the impulse, the resulting incoming wave $p^-(t)$ can be calculated with the following convolution integral:

$$p^-(t) = r * p^+(t). \quad (2)$$

Incidentally, mouthpiece pressure $p(t)$ and volume flow rate $U(t)$ have a relation with $p^\pm(t)$ as

$$p^\pm(t) = \frac{1}{2} [p(t) \pm Z_0 U(t)], \quad (3)$$

where Z_0 is the characteristic impedance of the plain wave and is equal to $Z_0 = \rho c / S$ with the air density ρ , the sound velocity c , and the cross-sectional area at the entrance of the instrument.

If the body of the clarinet can be regarded as a cylinder, the reflection function $r(t)$ is simply calculated with appropriate assumptions as shown in Fig. 4, where $2T$ is the time needed for sound to make a round trip between the entrance and the exit of the instrument.

2.3. Self-Excited Oscillation

Mouthpiece pressure $p(t)$ and volume flow rate $U(t)$ at present time t can be calculated with Eqs. (1) and (2). In practice, (two times the) pressure reflection wave

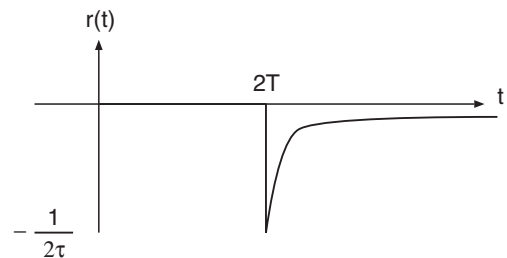


Fig. 4 Reflection function of a cylinder.

$$p_h(t) = \int_0^\infty r(s)[p(t-s) + Z_0U(t-s)]ds \quad (4)$$

is first calculated from past data of p and U . The equations

$$p(t) = Z_0U(t) + p_h, \quad (5)$$

$$U(t) = F(p(t)) \quad (6)$$

are, then, simultaneously solved to obtain $p(t)$ and $U(t)$.

Figure 3 also shows how to solve Eqs. (5) and (6) graphically. Lines (corresponding to Eq. (5)) with a slope of $1/Z_0$ and an intercept of p_h are drawn there. Intersections between the lines and the generator function specify the solutions of $p(t)$ and $U(t)$.

Generated pressure waveforms are illustrated in Fig. 5. At the beginning of the oscillation, p and U are positive. After the first reflection wave comes back to the mouthpiece, p_h becomes negative. p then becomes negative, and U is decreased. After the wave makes another round trip, p_h turns to positive. This leads to a positive p and an increase of U . During the repetition of these processes, the oscillation amplitude grows.

In the stationary state, the line represented by Eq. (5) scans the entire positive region of the generator function. When p takes the maximum value, the air flows upstream and U becomes negative. At the minimum value of p , the reed is closed completely and U vanishes. During the scanning, impulsive volume flows enter the instrument.

2.4. Energy Balance

By considering energy balance, we can understand the reason why amplitudes of $p(t)$ and $U(t)$ grow at the beginning of the oscillation. During dt , the air expelled from the player's mouth does work dW on the air column, which becomes

$$dW = \text{Force} \times \text{Distance} = p(t)A(t)dx(t), \quad (7)$$

where $dx(t)$ is the displacement of the edge of the air column (acoustic displacement), and $A(t)$ is the area of the

reed aperture. Dividing dW by dt yields work rate

$$\dot{W}(t) = p(t)A(t) \frac{dx(t)}{dt} = p(t)U(t). \quad (8)$$

Although $\dot{W}(t)$ becomes positive or negative at each time t , we consider total work during one oscillation period $\int_{(\text{one period})} p(t)U(t)dt$. If this quantity is positive, it means that the air gives energy to the air column. Amplitudes of $p(t)$ and $U(t)$ may then grow.

The above condition is satisfied if the oscillation phases of $p(t)$ and $U(t)$ are nearly the same. As shown in Fig. 3, the generator function has a positive slope near $p = 0$. This implies that $U(t)$ oscillates with the same phase as $p(t)$ as long as the amplitude is small. Therefore, the oscillation amplitude grows. The reason why the amplitude of $p(t)$ is saturated at p_0 is that the oscillation energy of the air column is lost due to negative U for p larger than p_0 .

2.5. Other Instruments

In brass instruments, the lips vibrate as a reed near the eigen frequency. This indicates that the dynamics of the lips should be considered. Therefore, the simplest model of the brass instrument can be obtained as a minor extension of the M-S-W model. Lip opening area $A(t)$ then becomes an independent variable in addition to $p(t)$ and $U(t)$. These are governed by Eqs. (1) and (2) and by an equation of the lip motion.

In air-jet driven instruments, such as the flue organ pipe, an air jet emerging from the flue exit, after traveling through the pipe mouth and being deflected by the sound, impinges on an edge (labium). A part of the airflow coming into the pipe $U_{\text{jet}}(t)$ excites air-column oscillation acoustically. Let the acoustic displacement at the pipe mouth be $Y(t)$. An infinitesimal fluctuation on the jet caused by the generated sound is propagated from the flue exit to the edge. The time needed for the propagation is set to τ . The generator function for the air jet driven instrument then becomes

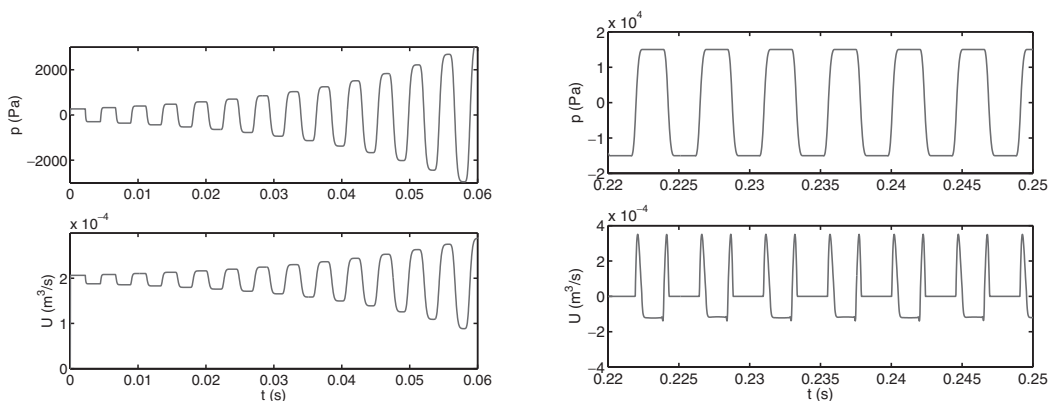


Fig. 5 Synthesized clarinet sound: Attack (left), Stationary state (right).

$$U_{\text{jet}}(t) = F(Y(t - \tau)), \quad (9)$$

where F is a monotone increasing function such as the hyperbolic tangent. Independent variables are $U(t)$, $U_{\text{jet}}(t)$, $Y(t)$ and $p(t)$ in this case. These are governed by Eqs. (2) and (9), $S\dot{Y}(t) = U(t)$ (S is the area of the pipe mouth), and an equation for acoustic radiation from the pipe mouth.

3. RECENT PROGRESS

3.1. Reed Instruments

Schumacher developed a physical model of the clarinet where the reed is regarded as a spring-mass system with one degree of freedom, and a reflection function calculated from the shape of an actual instrument is used [3]. This model can generate synthesized sound very similar to the actual one throughout the entire pitch range. More minute modeling of the reed vibration, such as that using a bending beam, has also been done [4,5]. Considering the resonance of the player's vocal tract, the former investigates the influence of the vocal tract on the quality of the generated sound. The latter successfully explains mechanisms of shifting pitch by the position of holding the reed between the lips and by the thickness of the reed.

In the double-reed instrument, pressure acting on the reed p_r is different from pressure at the entrance of the instrument p , since the reed and the instrument are not connected directly but via a narrow tube [6]. In the narrow tube, both pressure loss and recovery occur: the former is due to turbulence and the latter is to re-attachment of the flow to the tube wall. Experimental and theoretical analysis on this phenomenon has not been completed yet. Currently, it is modeled with a parameter Ψ in

$$p_r - p = \frac{1}{2} \rho \Psi \left(\frac{U}{S_r} \right)^2, \quad (10)$$

which relates p_r with p [7], where S_r is the cross-sectional area of the narrow tube. Due to Eq. (10), the generator function for the double-reed instrument differs from that for the single-reed instrument shown in Fig. 3. Estimations of the value of Ψ have been attempted [7,8].

3.2. Brass Instruments

By changing the embouchure and the blowing pressure, a brass player selects a resonance mode of the instrument to be excited for generating sound. The dynamics of the lip reed should, therefore, be appropriately modeled to understand the sounding principle of a brass instrument. By contrast with the reed of a woodwind instrument, Helmholtz inferred that the lips operated as a valve tending to open with a decrease in mouthpiece pressure (outward-striking model). Another possible modeling is that with a valve oscillating perpendicularly to the airflow as the vocal folds do (sideway-striking model). In this model, the lips

tend to close with a decrease in mouthpiece pressure because they are driven by Bernoulli pressure in the lip opening.

The two models provide different pitches of generated sound. The reason is as follows. First, (1) the lips oscillate near the eigen frequency. To maintain self-excited oscillation, therefore, the external force should be in the same direction of the velocity of lip oscillation. Second, (2) the acoustic load of the instrument is inductive for a frequency below a resonance frequency and capacitive for a frequency above it. For the outward-striking valve to satisfy condition (1), the mouthpiece pressure should take the minimum value at the moment when the lips move toward the mouthpiece with the maximum velocity. At this moment, the lip opening area increases from its average value, and the time-varying component of the volume flow rate increases from zero. This phase difference between the mouthpiece pressure and the volume flow, $\angle p - \angle U = -90^\circ$, can be achieved when the acoustic load is capacitive. From (2), sound generated by the outward-striking model has a fundamental frequency larger than a resonance frequency f_r . Similarly, sound generated by the sideway-striking model has a fundamental frequency smaller than f_r .

Which model simulates the actual lip vibration better? From simultaneous measurement of the mouthpiece pressure and the lip vibration with a strain gauge, Yoshikawa showed that the outward-striking model is better for the oscillation in the lower resonance modes, whereas the sideway-striking model is better in the higher resonance modes [9]. The same observations were made in stroboscopic measurement of lip vibration [10] and in a blowing experiment with a Helmholtz resonator [11]. In a physical modeling simulation [12], it was found that both of the one-dimensional models generate sound frequencies f_s far from (above or below depending on the models) a resonance frequency f_r , so an actual performance would be totally out of tune. This inconvenience was resolved by a two-dimensional model [13] where the lip is represented by one mass but has two degrees of freedom, for both outward and sideway vibrations. This model generates f_s , which is not very far from f_r , and also successfully replicates Yoshikawa's finding.

Toward a more minute model of the lip vibration, measurement has been done by various methods recently. One major trend is stroboscopic measurement of lip vibration [14,15], where surface waves on the lip called Rayleigh waves are observed. It is likely that the presence of the Rayleigh wave results in larger spectral levels in the higher frequency range. The other trend is artificial blowing experiments. Ehara *et al.* [16] measured the two-dimensional trajectory of an artificial lip. Another artificial lip developed by Gilbert *et al.* [17] was made of latex tubes filled with water and equipped with control devices for the

water pressure, mechanical pressure on the mouthpiece and blowing pressure. In an experiment with a similar apparatus [18], it was found that the lip has more than one eigen mode by driving the lips with external sound. Vilain *et al.* [19] measured the lip vibration frequency and minimum blowing pressure necessary to maintain oscillation as functions of water pressure. They concluded that a model having at least four degrees of freedom is needed for consistency with their measurements.

As for computer simulation, self-excited oscillations were successfully simulated with a two-dimensional finite element model of the lip [20]. If this simulation is extended to that in three dimension, A detailed comparison with the measurement would be possible. For this extension, it would probably be necessary to model the three-dimensional airflow around the lips. To deal with the coupling between mechanical oscillation of the lips and the airflow in three dimensions, highly advanced methods in numerical analysis would be required.

3.3. Air-Jet Driven Instruments

The model shown in section 2.5 generates sound at a level at least 10 dB larger than the actual sound pressure level. Fabre *et al.* [21] showed that this is because the energy dissipation is ignored in vortex shedding at the edge by the acoustic flow. Adopting this effect, Verge *et al.* [22] proposed a model of the recorder. This model has another improvement in that the air jet is considered to excite the pipe acoustically as a dipole source. This model can successfully replicate sound generated in the recorder. Since the late 90's, research in the air-jet driven instrument has entered a phase of major change toward a rigorous aerodynamic description.

Deflection of the jet by sound is the crucial part in the sounding principle of the air-jet driven instrument. The generator function in Eq. (9) can be easily obtained from a jet deflection theory. Currently, the theory proposed by Fletcher [23] is most widely accepted. This theory successfully predicts fundamental properties of the instrument such as overblowing behavior with a change in blowing pressure [24,25], although it is constructed based on many conceptual approximations.

According to the linear stability analyses [26–28], an infinitesimal disturbance on a jet of infinite length in an inviscid fluid grows exponentially with the growth coefficient μ and is propagated with the phase velocity V_{ph} . In Fletcher's theory, this property of the hypothetical jet is applied to an actual jet emerging horizontally (in the x -direction) from the flue slit. In addition, the following assumptions are made: (1) The jet is superimposed on the acoustic displacement $Y(t)$ that oscillates sinusoidally in the pipe mouth. (2) However, the jet deflection displacement $\eta(x, t)$ satisfies a boundary condition $\eta(0, t) = 0$ at the

flue exit. Then, $\eta(x, t)$ becomes

$$\eta(x, t) = Y(t)[1 - e^{\mu x} e^{-i\omega x/V_{ph}}], \quad (11)$$

where the first term in the brackets indicates that the jet oscillates with $Y(t)$, and the second term indicates that a disturbance on the jet $-Y(t)$ at the flue exit $x = 0$ grows exponentially while the jet travels, as the linear stability analysis suggests.

Several attempts have been made to understand the jet deflection from an aerodynamic point of view [29,30]. Complex motion of a jet deflected by sound, which can not be predicted by Eq. (11), has been revealed by measurement of the deflection amplitude by hot-wire anemometry [31] and visualization [32,33]. The effects of the flue geometry [34] and the edge angle [35] on the stability of the jet deflection have been investigated in flow visualization experiments. Recently, an edgetone theory by Holger *et al.* [36] has drawn attention as a means of analyzing the jet deflection. In a recent experiment [37] on flow visualization with the Schlieren technique, jet deflection amplitude was analyzed both with Fletcher's and Holger's theories.

Numerical analysis of a jet with computational fluid dynamics has become realistic recently. Consequently, a two-dimensional simulation of a flue instrument [38] has been developed to a three-dimensional one [39]. An edgetone simulation in three dimensions [40] would also be promising for analyzing the jet deflection. On the other hand, a two-dimensional simulation of a deflected jet [41] has been done with reasonable accuracy as judged by measurement of the jet under the same conditions.

4. CONCLUSIONS

The principles of sound production in wind instruments were outlined using a simple physical model by McIntyre, Schumacher and Woodhouse. Recent progress was separately reviewed for each type of wind instrument. We found that three different phenomena are involved in sounding: mechanical oscillation of a reed, airflow dynamics, and acoustic resonance of the instrument. Until recently, these have been discussed in many cases with lumped models with only a few degrees of freedom. Except for acoustic resonance, multi-dimensional models with a large degree of freedom would be needed to further investigate the sound production mechanisms. Due to rapid development of measurement techniques and computer simulation, it has become easier to investigate and to reconstruct the details of these phenomena in multiple dimensions. However, it still takes physical insight to understand the essence of sound production, as well as clarity in aiming toward targets of what to explain and to what extent.

REFERENCES

- [1] A. Hirschberg, J. Gilbert, R. Msallam and A. P. J. Wijnands, "Shock waves in trombones," *J. Acoust. Soc. Am.*, **99**, 1754–1758 (1996).
- [2] M. E. McIntyre, R. T. Schumacher and J. Woodhouse, "On the oscillations of musical instruments," *J. Acoust. Soc. Am.*, **74**, 1325–1345 (1983).
- [3] R. T. Schumacher, "Ab Initio Calculations of the Oscillations of a Clarinet," *Acustica*, **48**, 71–85 (1981).
- [4] S. D. Sommerfeldt and W. J. Strong, "Simulation of a player-clarinet system," *J. Acoust. Soc. Am.*, **83**, 1908–1918 (1988).
- [5] I. Miyachi and Y. Takasawa, "A vibration analysis of clarinet reed," *Tech. Rep. Musical Acoust. Acoust. Soc. Jpn.*, MA00-17, pp. 3–10 (2000).
- [6] A. P. J. Wijnands and A. Hirschberg, "Effect of a pipe neck downstream of a double reed," *Proc. Int. Symp. Musical Acoustics*, Dourdan, France, pp. 149–152 (1995).
- [7] C. Vergez, A. Almeida, R. Caussé and X. Rodet, "Toward a simple physical model of double-reed musical instruments: Influence of aero-dynamical losses in the embouchure on the coupling between the reed and the bore of the resonator," *Acta Acustica/Acustica*, **89**, 964–973 (2003).
- [8] A. Almeida, C. Vergez, R. Caussé and X. Rodet, "Physical model of an oboe: comparison with experiments," *Proc. Int. Symp. Musical Acoustics*, Nara, Japan, pp. 112–115 (2004).
- [9] S. Yoshikawa, "Acoustical behavior of brass player's lips," *J. Acoust. Soc. Am.*, **97**, 1929–1939 (1995).
- [10] D. C. Copley and W. J. Strong, "A stroboscopic study of lip vibrations in a trombone," *J. Acoust. Soc. Am.*, **99**, 1219–1226 (1996).
- [11] F.-C. Chen and G. Weinreich, "Nature of the lip reed," *J. Acoust. Soc. Am.*, **99**, 1227–1233 (1996).
- [12] S. Adachi and M. Sato, "Time-domain simulation of sound production in the brass instrument," *J. Acoust. Soc. Am.*, **97**, 3850–3861 (1995).
- [13] S. Adachi and M. Sato, "Trumpet sound simulation using a two-dimensional lip vibration model," *J. Acoust. Soc. Am.*, **99**, 1200–1209 (1996).
- [14] R. D. Ayers, "New perspective on the brass instruments," *Proc. Int. Symp. Musical Acoustics*, Leavenworth, USA, pp. 129–134 (1998).
- [15] S. Yoshikawa and Y. Muto, "Lip-wave generation in horn players and the estimation of lip-tissue elasticity," *Acta Acustica/Acustica*, **89**, 145–162 (2003).
- [16] F. Ehara, K. Nagai and K. Mizutani, "Analysis of two-dimensional vibrations of lips in an artificial brass-playing system using optical measurements and numerical calculations," *J. Acoust. Soc. Jpn. (J)*, **59**, 541–549 (2003).
- [17] J. Gilbert, S. Ponthus and J.-F. Petiot, "Artificial buzzing lips and brass instruments: Experimental results," *J. Acoust. Soc. Am.*, **104**, 1627–1632 (1998).
- [18] J. S. Cullen, J. Gilbert and D. M. Campbell, "Brass instruments: Linear stability analysis and experiments with an artificial mouth," *Acustica/Acta Acustica*, **86**, 704–724 (2000).
- [19] C. E. Vilain, X. Pelorson, A. Hirschberg, L. Le Marrec, W. Op't Root and J. Willems, "Contribution to the physical modeling of the lips. Influence of the mechanical boundary conditions," *Acta Acustica/Acustica*, **89**, 882–887 (2003).
- [20] D. O. Ludwigsen, "Physical modeling of the trombone player's lips," *Proc. Stockholm Music Acoustics Conf.*, Stockholm, Sweden, pp. 209–212 (2003).
- [21] B. Fabre, A. Hirschberg and A. P. J. Wijnands, "Vortex shedding in steady oscillations of a flue organ pipe," *Acustica*, **82**, 863–877 (1996).
- [22] M. P. Verge, A. Hirschberg and R. Caussé, "Sound production in recorderlike instruments. II. A simulation model," *J. Acoust. Soc. Am.*, **101**, 2925–2939 (1997).
- [23] N. H. Fletcher and S. Thwaites, "Wave propagation on an acoustically perturbed jet," *Acustica*, **42**, 323–334 (1979).
- [24] N. H. Fletcher, "Sound production by organ flue pipes," *J. Acoust. Soc. Am.*, **60**, 926–936 (1976).
- [25] S. Adachi, "Time-domain modeling and computer simulation of an organ flue pipe," *Proc. Inst. Acoust.*, **19**, 251–260 (1997).
- [26] Lord Rayleigh, *The Theory of Sound* (Macmillan, New York, Reprinted by Dover, New York, 1945), Vol. 2, pp. 376–414.
- [27] P. G. Drazin and L. N. Howard, "Hydrodynamic stability of parallel flow of inviscid fluid," *Adv. Appl. Mech.*, **9**, 1–89 (1966).
- [28] G. E. Mattingly and W. O. Criminale, Jr., "Disturbance characteristics in a plane jet," *Phys. Fluids*, **14**, 2258–2264 (1971).
- [29] B. Fabre and A. Hirschberg, "Physical modeling of flue instruments: A review of lumped models," *Acustica/Acta Acustica*, **86**, 599–610 (2000).
- [30] B. Fabre and A. Hirschberg, "From sound synthesis to instrument making: An overview of recent researches on woodwinds," *Proc. Stockholm Music Acoustics Conf.*, Stockholm, Sweden, pp. 239–242 (2003).
- [31] A. W. Nolle, "Sinuous instability of a planar air jet: Propagation parameters and acoustic excitation," *J. Acoust. Soc. Am.*, **103**, 3690–3705 (1998).
- [32] S. Yoshikawa, "Jet-wave amplification in organ pipes," *J. Acoust. Soc. Am.*, **103**, 2706–2717 (1998).
- [33] S. Yoshikawa, "A pictorial analysis of jet and vortex behaviours during attack transients in organ pipe models," *Acustica/Acta Acustica*, **86**, 623–633 (2000).
- [34] C. Ségoufin, B. Fabre, M. P. Verge, A. Hirschberg and A. P. J. Wijnands, "Experimental study of the influence of the mouth geometry on sound production in a recorder-like instrument: windway length and chamfers," *Acustica/Acta Acustica*, **86**, 649–661 (2000).
- [35] S. Dequand, J. F. H. Willems, M. Leroux, R. Vullings, M. van Weert, C. Thieulot and A. Hirschberg, "Simplified models of flue instruments: Influence of mouth geometry on the sound source," *J. Acoust. Soc. Am.*, **113**, 1724–1735 (2003).
- [36] D. Holger, T. Wilson and B. Beavers, "Fluid mechanics of the edgetone," *J. Acoust. Soc. Am.*, **62**, 1116–1128 (1977).
- [37] P. de la Cuadra and B. Fabre, "Analysis of jet instability in flute-like instruments by means of image processing: effect of the excitation amplitude," *Proc. Int. Symp. Musical Acoustics*, Nara, Japan, pp. 246–250 (2004).
- [38] P. Skordos and G. Saussman, "Comparison between subsonic flow simulation and physical measurements of flue pipes," *Proc. Int. Symp. Musical Acoustics*, Dourdan, France, pp. 79–85 (1995).
- [39] H. Kühnelt, "Simulating the sound generation in flutes and flue pipes with the Lattice-Boltzmann-Method," *Proc. Int. Symp. Musical Acoustics*, Nara, Japan, pp. 251–254 (2004).
- [40] S. Ito, T. Fujisawa and G. Yagawa, "Computational fluid analysis of the sound generation mechanism of air-reed instruments," *Tech. Rep. Musical Acoust. Acoust. Soc. Jpn.*, MA2001-61, pp. 1–6 (2002).
- [41] S. Adachi, "CFD analysis of air jet deflection — Comparison with Nolle's measurements," *Proc. Stockholm Music Acoustics Conf.*, Stockholm, Sweden, pp. 313–316 (2003).